Human Cancer Biology

Clinical Cancer Research

DNA Copy Numbers Profiles in Affinity-Purified Ovarian Clear Cell Carcinoma

Kuan-Ting Kuo[1,2], Tsui-Lien Mao[2], Xu Chen[1,3], Yuanjian Feng[4], Kentaro Nakayama[5], Yue Wang[4], Ruth Glas[6], M. Joe Ma[7], Robert J. Kurman[1], Ie-Ming Shih[1], and Tian-Li Wang[1]

Abstract

Purpose: Advanced ovarian clear cell carcinoma (CCC) is one of the most aggressive ovarian malignancies, in part because it tends to be resistant to platinum-based chemotherapy. At present, little is known about the molecular genetic alterations in CCCs except that there are frequent activating mutations in *PIK3CA*. The purpose of this study is to comprehensively define the genomic changes in CCC based on DNA copy number alterations.

Experimental Design: We performed 250K high-density single nucleotide polymorphism array analysis in 12 affinity-purified CCCs and 10 CCC cell lines. Discrete regions of amplification and deletion were also analyzed in additional 21 affinity-purified CCCs using quantitative real-time PCR.

Results: The level of chromosomal instability in CCC as defined by the extent of DNA copy number changes is similar to those previously reported in low-grade ovarian serous carcinoma but much less than those in high-grade serous carcinoma. The most remarkable region with DNA copy number gain is at chr20, which harbors a potential oncogene, *ZNF217*. This discrete amplicon is observed in 36% of CCCs but rarely detected in serous carcinomas regardless of grade. In addition, homozygous deletions are detected at the *CDKN2A/2B* and *LZTS1* loci. Interestingly, the DNA copy number changes observed in fresh CCC tissues are rarely detected in the established CCC cell lines.

Conclusions: This study provides the first high resolution, genome-wide view of DNA copy number alterations in ovarian CCC. The findings provide a genomic landscape for future studies aimed at elucidating the pathogenesis and developing new target-based therapies for CCCs. *Clin Cancer Res; 16(7); 1997–2008. ©2010 AACR.*

Ovarian cancer is a heterogeneous group of neoplastic diseases that are thought to arise from the epithelial cells of the fallopian tube, ovarian surface inclusion cysts, or endometriosis (1). They are classified into serous, mucinous, endometrioid, and clear cell types corresponding to the different types of epithelia in the organs of the female reproductive tract (2–4). Correlated with their respective clinical behaviors, each of these histologic types is further divided into three groups: benign (cystadenoma), intermediate (borderline tumor), and malignant (carcinoma; ref. 2). Clear cell carcinoma of the ovary (CCC) is characterized by distinct morphologic features and clinical behavior. Although CCC represents <10% of ovarian cancers in the United States, it appears to occur more frequently in Asia. Previous clinicopathologic studies have indicated that CCC develops in a stepwise fashion from endometriosis, atypical endometriosis to CCC (5–7). In general, most CCCs are indolent, typically presenting at early stage when surgical intervention is effective in eradicating the disease. However, in advanced stage, CCC is usually resistant to conventional chemotherapy and highly aggressive (8, 9). Little is known about the pathogenesis of CCC, thus a better understanding of which holds the promise of development of new and more effective therapies is needed (9–15). At present one of the most significant molecular genetic changes described in CCC is the frequent somatic activating mutation of *PIK3CA* (16), which were detected in ~48% of affinity-purified fresh tumors and cell lines. On the other hand, the frequency of *PIK3CA* mutations is relatively low in

Authors' Affiliations: [1]Division of Gynecological Pathology, Departments of Pathology, Gynecology/Obstetrics, and Oncology, Johns Hopkins University School of Medicine, Baltimore, Maryland; [2]Department of Pathology, National Taiwan University Hospital, Medical College, National Taiwan University, Taipei, Taiwan; [3]Department of Urology, Union Hospital, Tongji Medical College, Huazhong University of Science and Technology, Wuhan, China; [4]Bradley Department of Electrical and Computer Engineering, Virginia Polytechnic Institute and State University, Arlington, Virginia; [5]Department of Gynecology and Obstetrics, Shimane University, Izumo, Japan; [6]Division of Hematology/Oncology, David Geffen School of Medicine, University of California at Los Angeles, Los Angeles, California; and [7]Department of Pathology, Florida Hospital, Orlando, Florida

Note: Supplementary data for this article are available at Clinical Cancer Research Online (http://clincancerres.aacrjournals.org/).

K-T. Kuo, T-L. Mao, and X. Chen contributed equally to this work.

Corresponding Authors: Tian-Li Wang, Johns Hopkins University School of Medicine, CRBII, 1550 Orleans Street, Room 306, Baltimore, MD 21231. Phone: 410-502-0863; Fax: 410-502-7943; E-mail: tlw@jhmi.edu or Ie-Ming Shih, Johns Hopkins University, CRBII, 1550 Orleans Street, Room 305, Baltimore, MD 21231. Phone: 410-502-7774; E-mail: shihie@yahoo.com.

doi: 10.1158/1078-0432.CCR-09-2105

Translational Relevance

Clear cell carcinoma of the ovary (CCC) is characterized by distinct morphologic features and clinical behavior. In general, most CCCs are indolent, typically presenting in one ovary (stage I) when surgical intervention is effective in eradicating the disease. However, in advanced stage, CCC can be highly aggressive because of its resistance to conventional chemotherapy. Therefore, a better understanding of the pathogenesis of CCC could assist in the development of new therapeutic approaches for this disease. The current study is the first report describing the genomic landscapes of the CCCs using tumor cells purified from fresh cancerous tissue and high-density single nucleotide polymorphism array. The unique molecular genomic alterations of CCC as described herein will be very useful in future studies aimed at elucidating the pathogenesis of CCC and in the development of target-based therapeutics for this aggressive ovarian neoplasm.

high-grade serous carcinoma and the other major types of ovarian cancer. In contrast, CCC has a significantly lower frequency of *TP53* mutations than high-grade serous carcinomas, which harbor this mutation in over 50% of cases.

Besides these observations in a few specific genes, the genomic landscape of CCC is poorly understood. Alterations in DNA copy number is a cardinal feature of carcinogenesis and identification of amplified or deleted genes would be important in elucidating the molecular pathogenesis of CCC. In this study, we applied a high-resolution single nucleotide polymorphism (SNP) array to analyze genome-wide DNA copy number changes in CCC. To enhance the sensitivity and specificity of our analysis, we used affinity-purified tumor cells prepared from fresh surgical specimens in addition to established cell lines. Our data revealed a distinct pattern of DNA copy number changes in CCC compared with high-grade and low-grade ovarian serous carcinoma. More importantly, we identified the *ZNF217* locus as the most commonly amplified region in CCC.

Materials and Methods

Tumor specimens. Tissue samples from ovarian CCCs were freshly collected from the Department of Pathology at the Johns Hopkins Hospital and the National Taiwan University Hospital. Tumor cells were affinity purified by anti-BerEP4–conjugated magnetic beads as previously described (17). The acquisition of the anonymous tissue specimens for this study was approved by the Institutional Review Boards of participant institutions. Their clinical disease stages and mutational profiles of the clinical samples were shown in Table 1. In addition, genomic DNA of the same batch of DNA isolation from 10 CCC cell lines used in our previous study were included as controls (16). The CCC cell lines were maintained in the University of California at Los Angles in Dr. R. Glas and Dr. D. Slamon's laboratory. The cell lines ES2 and TOV21G were obtained from the American Type Culture Collection. The cell lines OVISE, OVMANA, OVTOKO, and RMG1 were obtained from the Japanese Health Science Research Resources Bank. OV207 was a kind gift from Dr. V. Shridhar, Mayo Clinic, Rochester, MN. OVCA429 was a kind gift from Dr. B. Karlan, Cedars Sinai, Los Angeles, California and this line was initially described as a serous tumor, but later studies showed phenotypes close to CCC (18–20). JHOC5 was a kind gift of Dr. Kentaro Nakayama, Shimane University, Shimane, Japan. Individuality of each cell line was checked by mitochondrial DNA sequencing.

SNP array analysis. SNPs were genotyped using 250K StyI arrays (Affymetrix) in the Microarray Core Facility at the Dana-Farber Cancer Institute. A detailed protocol is available at the Core center Web page.[8] Briefly, genomic DNA was cleaved with the restriction enzyme StyI and ligated with linkers, followed by PCR amplification. The PCR products were purified and then digested with DNaseI to a size ranging from 250 to 2,000 bp. Fragmented PCR products were then labeled with biotin and hybridized to the array. Arrays were then washed on the Affymetrix fluidics stations. The bound DNA was then fluorescently labeled using streptavidin-phycoerythrin conjugates and scanned using a confocal laser scanner.

dChip software (version 2006) was used to analyze the SNP array data as previously described (21). Data were normalized to a baseline array with median signal intensity at the probe intensity level using the invariant set normalization method. A model-based (PM/MM) method was used to obtain the signal value for each SNP in each array. Signal values for each SNP were compared with the average intensities from 12 normal samples. To infer the DNA copy number from the raw signal data, we used the Hidden Markov Model based on the assumption of diploidy for normal samples. Mapping information of SNP locations and cytogenetic band were based on the curation of Affymetrix and ensemble National Center for Biotechnology Information Build 36.1 (March 2006, hg18). Amplification was defined as a cutoff value of >3.0 copies in more than six consecutive SNPs. A cutoff of <0.69 copy was used to define homozygous deletion. If there were intermittent, nonconsecutive probes with inferred copy numbers that deviated less than ±0.1 copies from the cutoff criteria, this probe was considered within the cutoff range. The boundary of amplification and deletion was visually inspected and determined if difference between franking probes is >50%.

Chromosome instability index. To facilitate the quantification of subchromosomal copy number alterations, we applied the Circular Binary Segmentation algorithm to determine the levels of DNA copy number changes

[8] http://biosun1.harvard.edu/

Table 1. Summary of mutation result in CCCs

Clinical samples used in SNP array analysis

TCS no.	Stage	CDKN2A/B	ZNF217	TP53	KRAS/BRAF	PIK3CA
1021	IV	No HD	No AMP	Wt	Wt	546 Q>K (1636 C>A)
321	IC	No HD	AMP	Wt	Wt	Wt
1202	IIIC	No HD	AMP	Wt	Wt	542 E>K (1624 G>A)
516	IIIC	No HD	AMP	Wt	Wt	Wt
797	IIIB	No HD	No AMP	Wt	Wt	1047 H>R (3140 A>G)
JM8	IA	No HD	AMP	Wt	Wt	Wt
8T	IC	No HD	No AMP	NP	Wt	Wt
1T	IC	No HD	No AMP	NP	NP	NP
7T	IA	No HD	No AMP	NP	Wt	1047 H>R (3140 A>G)
192	IC	No HD	No AMP	Wt	Kras 12 G>D (35 G>A)	Wt
392	IV	HD	No AMP	199 G>V (596 G>T)	Kras 12 G>D (35 G>A)	Wt
750	IV	No HD	AMP	Wt	Wt	1047 H>R (3140 A>G)

Cell lines used in SNP array analysis

TCS NO	Stage	CDKN2A/B	ZNF217	TP53	KRAS/BRAF	PIK3CA
OV207	Cell line	No HD	No AMP	273 R>H (818 G>A)	Wt	Wt
OVCA429	Cell line	No HD	No AMP	Wt	Wt	545 G>A (1633 G>A)
OVISE	Cell line	No HD	No AMP	Wt	Wt	Wt
OVMANA	Cell line	No HD	AMP	Wt	Wt	545 E>V (1634 A>T)
OVTOKO	Cell line	No HD	No AMP	Wt	Wt	Wt
RMG1	Cell line	No HD	No AMP	Wt	Wt	Wt
TOV21G	Cell line	No HD	No AMP	Wt	Kras 13 G>C (37 G>T)	1047 H>Y (3139 C>T)
JHOC5	Cell line	HD	No AMP	Wt	Wt	Wt
ES2	Cell line	No HD	No AMP	241 S>F (722 C>T)	Braf 600 V>E (1799 T>A)	Wt
KK	Cell line	No HD	No AMP	Wt	Wt	545 E>A (1634 A>C)

Independent clinical samples used in qPCR analysis

Sample no.	Stage	CDKN2A/B	ZNF217	TSHZ2	BCAS1
1	IA	No HD	No AMP	No AMP	No AMP
2	IA	No HD	No AMP	No AMP	No AMP
3	IC	No HD	No AMP	AMP	No AMP
4	IC	No HD	AMP	No AMP	No AMP
5	IC	No HD	No AMP	No AMP	No AMP
6	IC	HD	AMP	AMP	No AMP
7	IC	No HD	No AMP	No AMP	No AMP
8	IC	No HD	No AMP	No AMP	No AMP
9	IC	No HD	No AMP	No AMP	No AMP
10	IC	No HD	No AMP	No AMP	No AMP
11	IC	No HD	AMP	AMP	No AMP
12	IC	No HD	AMP	No AMP	No AMP
13	IIC	No HD	No AMP	No AMP	No AMP
14	IIIB	No HD	No AMP	No AMP	No AMP
15	IIIC	No HD	AMP	No AMP	No AMP
16	IIIC	No HD	No AMP	No AMP	No AMP
17	IIIC	No HD	AMP	AMP	No AMP
18	IIIC	No HD	No AMP	NA	NA
19	Recurrent	No HD	No AMP	No AMP	No AMP
20	Recurrent	No HD	No AMP	No AMP	AMP
21	Recurrent	HD	AMP	AMP	AMP

*HD, homozygous deletion; AMP, amplification; NP, not performed; Wt, wild type.

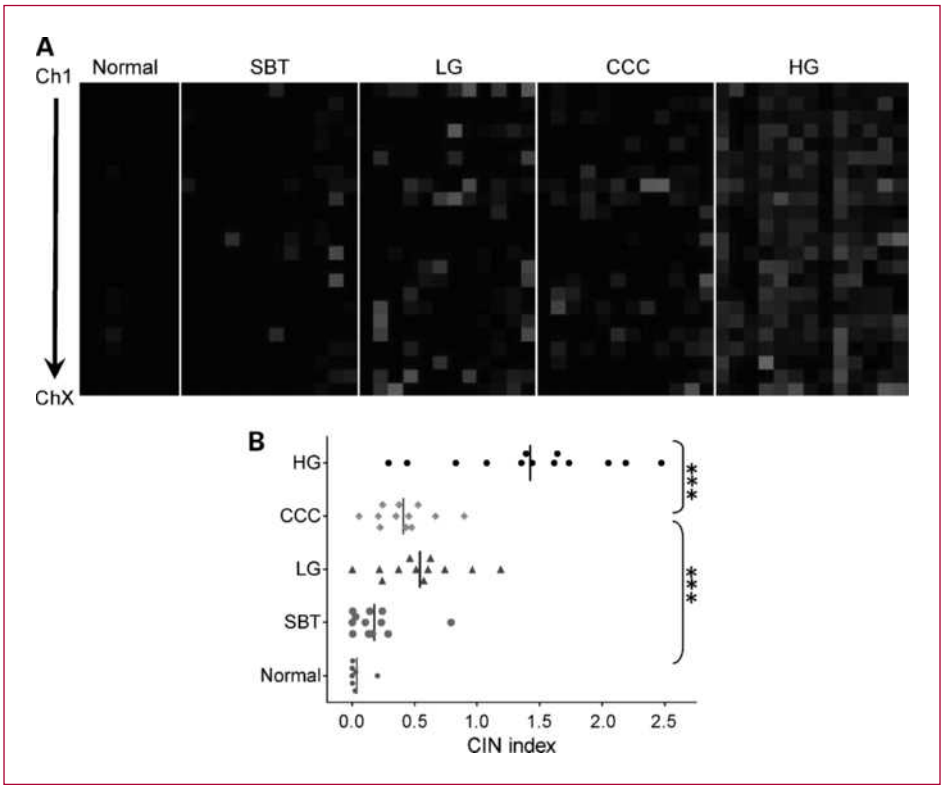

Fig. 1. Genome-wide CIN index in ovarian CCCs. A, the CIN index in individual chromosome of each serous tumor is plotted using a pseudocolor gradient indicating the copy number alteration level (low to high, dark to red). SBT, serous borderline tumor (atypical proliferative serous tumor); LG, low-grade serous carcinoma; HG: high-grade serous carcinoma. B, genome-wide CIN index for each tumor. The CIN index of high-grade serous carcinomas is significantly higher than CCC. CIN index of CCC is significantly higher than its adjacent normal stromal fibroblasts. ***, $P < 0.001$.

and the outcome is represented as chromosome instability index (CIN). The computation for CIN index was described in one of our previous studies (22). Briefly, the chromosome-specific CIN index is defined as the sum of amplitudes of all gain/loss segments divided by the total number of SNPs in the chromosome, and the genome-wide CIN index was defined as log(C1+1) + … + log (*Ci* + 1) + … + log(C23 + 1), in which *Ci* is the CIN index of chromosome i. For a gain segment, the amplitude is the average intensity of SNP signals within the segment. For a loss segment, to match the effect of losses to the same scale of gains, the amplitude is calculated by $2.5 + (A - 2.5)(1.5 - a)/1.5$, in which "*a*" is the average intensity of SNP signals within the loss segment and "*A*" is the maximum gain amplitude across all cases in the same chromosome.

Quantitative real-time PCR. The gDNA copy number of the candidate genes was validated by quantitative real-time PCR using an iCycler (Bio-Rad) with SYBR green dye (Molecular Probes). Averages in the threshold cycle number of triplicate measurements were obtained. The results were expressed as the difference between the threshold cycle number of the gene of interest and the threshold cycle number of a *Line-1* gene for which gDNA copy number is relatively constant among tumor samples (23). cDNA copy number was measured using the same procedure except the relative copy number of each candidate gene was normalized to the copy number of *APP*, a gene that mRNA expression is constant among samples (24).The primer sequences are listed in Supplementary Tables S1 and S2.

Transfection and biological effects of* ZNF217 *small interfering RNA treatment. Synthetic small interfering RNA (siRNA) targeting ZNF217 and Luciferase were purchased from Dharmacon and they were used to transfect CCC cell lines using Lipofectamine 2000 (Invitrogen). Two different siRNAs were found to efficiently knock down ZNF217, and their sequences are GAACAGAACCUCCCAAGGA and GAGGAUGCCUUGUCAAUGA. siRNA for Luciferase (UAAGGCUAUGAAGAGAUAC) was used as a control. Following transfection, cells were seeded into 96-well plates and the relative cell number was measured by the SYBR Green reagent (Invitrogen) using a fluorescent microplate reader. Data were expressed as mean ± 1 SD from five replicates in each experimental group. Early apoptosis was detected by measuring the caspase-3/7 activity using a kit purchased from Promega. The uptake of bromodeoxyuridine (BrdUrd) was used as an indicator for cell proliferation. In brief, 24 to 96 h after transfection, cells were incubated with 10 μmol/L BrdUrd for 1 h, fixed with methanol, and immunostained with an anti-BrdUrd antibody following the protocol provided in a kit (RPN202, GE Healthcare). The percentage of BrdUrd-positive cells was determined by counting ~300 cells from each well. The data were expressed as mean ± 1 SD from triplicate wells.

Statistic analysis. The differences in parameters were determined by Mann-Whitney nonparametric test for data presented in Fig. 1B, and *P* value was determined by two-tailed analysis. Paired *t* test was done to determine the significance of difference in the CIN index between matched normal and tumor samples. Fisher's

exact test was done to determine the correlation of *ZNF217* amplification and stage. Unpaired *t* test was done for the data presented in Fig. 5. The significant level (α) was set at 0.05 (*, $P < 0.05$; **, $P < 0.01$; and ***, $P < 0.001$).

Results

The chromosomal instability level in CCCs. The level of CIN in CCC was assessed according to the degree and extent of changes in DNA copy number in all chromosomes. The CIN index was used to quantify the CIN level and was developed based on the sum of amplitude in each gain or loss region, normalized to the total SNP probe numbers for each chromosome (22). The CIN index was first compared between tumor stromal fibroblasts and the epithelium in the carcinomas isolated from seven CCCs. The results showed that the CIN index of the stromal cells consistently approached zero in all chromosomes, whereas the carcinoma showed an elevated CIN index. Paired *t* test indicated the CIN index was significantly elevated in carcinomatous component compared with the matched tumor-associated stromal fibroblasts ($P < 0.01$) as internal controls. Next, CIN indices of CCCs were compared with those from affinity-purified ovarian serous borderline tumors, low-grade serous carcinomas, and high-grade serous carcinomas

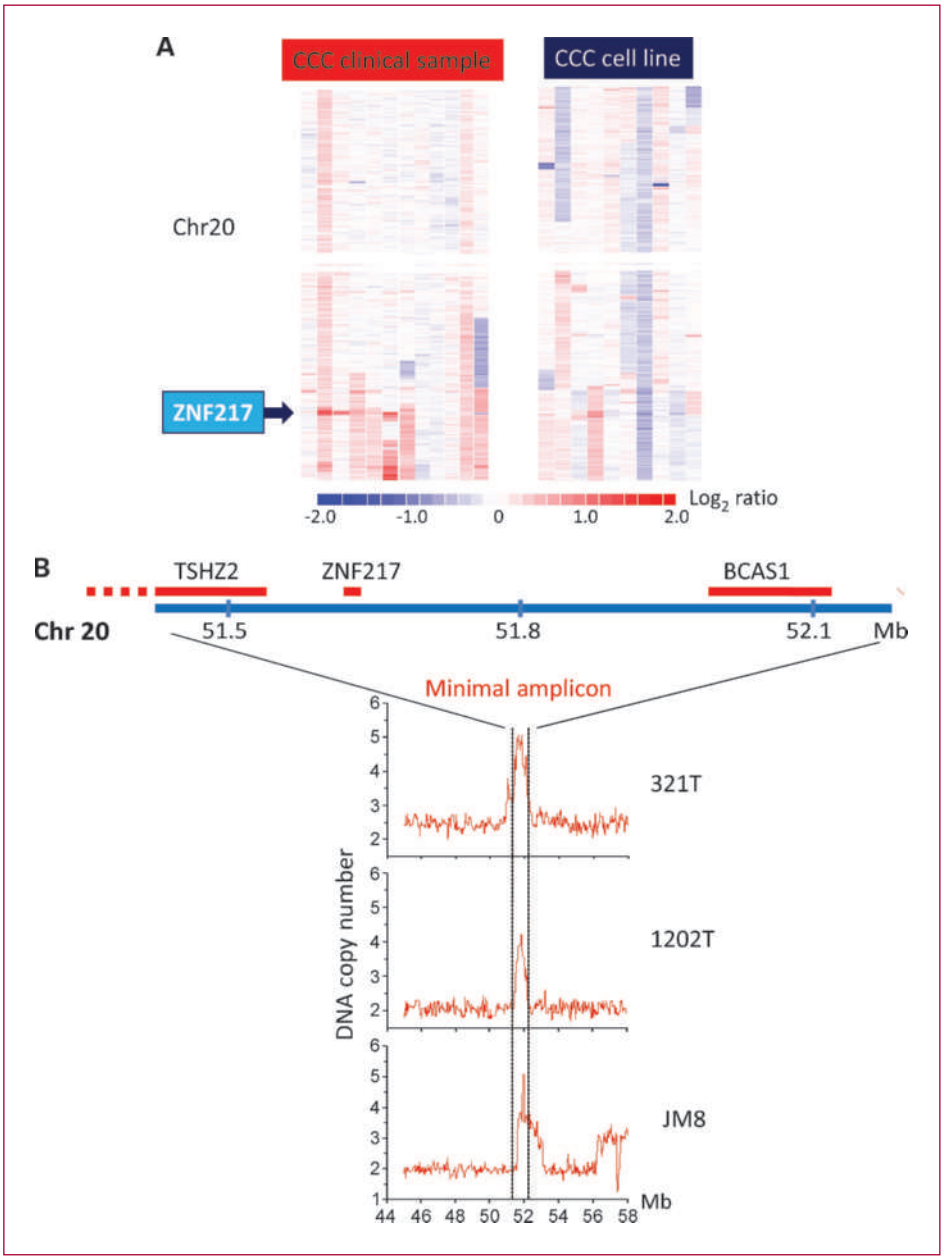

Fig. 2. Copy number alteration in chromosome 20. A, DNA copy number changes are represented as pseudocolor gradients corresponding to the copy number increase (red boxes) and decrease (blue boxes) compared with pooled normal samples. Each column represents an individual tumor sample. Arrow, amplification of ZNF217 region. B, aligning three tumors with discrete amplicon at chr20q13.2 delineates a minimal amplification region (dotted lines).

previously reported (22). The results show that CIN indices in CCCs were similar to those in low-grade serous carcinomas but were higher than those in serous borderline tumors and lower than those in high-grade serous carcinomas. Figure 1 lists the genome-wide CIN indices in all CCCs analyzed together with those in different types of ovarian serous tumors. Specifically, Fig. 1A includes the CIN indices at each chromosome and Fig. 1B includes the genome-wide CIN indices (the combined CIN indices from all chromosomes) in each specimen. These findings indicate that although CCC as a group has an elevated level of genomic instability compared with associated nonneoplastic stromal tissue, its CIN level is relatively modest compared with that found in high-grade serous carcinoma.

Amplification of the* ZNF217 *locus in CCCs. Although the genomic landscape of DNA copy number in CCC is relatively "flat" when compared with high-grade serous carcinoma, there are several discrete DNA copy number gains and losses. Among them, the most remarkable amplification found in the affinity-purified CCC samples is the DNA copy number gain at the chr20q13.2 locus (Fig. 2A). Five of the 12 cases analyzed are found to harbor this genomic amplification with peak amplitude ranges from 3.8 to 5.1 copies. To delineate the minimal amplified region, we aligned the amplified locus in three cases with discrete amplification and the minimal amplified region is determined to be between chr20:51,428,300 and 52,180,900 bp (Fig. 2B). Only three genes (*TSHZ2*, *ZNF217*, and *BCAS1*) are located within this minimal amplified region, including a previous reported potential oncogene *ZNF217*, which is amplified in breast and gastric carcinomas (25, 26). To determine the amplification frequency at this locus, we performed quantitative PCR in an additional 21 CCCs and found 7 of them with *ZNF217* DNA copy number gain (Table 1). Quantitative PCR was also done to determine the amplification frequency of the other two franking genes in 20 of the 21 samples. The results showed that *TSHZ2* is amplified in 5 of 20 cases, whereas *BCAS1* is amplified in 2 of 20 cases. In sum, by combining data from SNP array and qPCR analyses, *ZNF217* showed the highest amplification frequency, which occurred in 12 (36%) of 33 CCCs.

To determine if the amplification of chr20q13.2 leads to transcript upregulation, we performed quantitative real-time PCR to analyze gDNA and cDNA copy number in 20 of the 33 CCC samples for all three genes within the minimal amplicon. The 20 cases were selected because both their gDNA and cDNA samples from the same cases were available for analysis. The results showed that there was a positive correlation between genomic DNA copy number and *ZNF217* transcript number with an R value of 0.61 ($P < 0.01$, Spearman test; Table 2), whereas there was no significant correlation of either *TSHZ2* or *BCAS1*.

In addition to the amplification in the chr20q13.2 locus, low levels of chromosomal gain encompassing large chromosomal regions were observed in chr8q (Fig. 3) as well as chr17q (Supplementary Fig. S1; Fig. 4). However, these regions are relatively large and contain numerous genes that preclude the identification of a candidate driver oncogene(s) at this moment.

Table 2. Correlation of ZNF217 genomic DNA and mRNA copy numbers

Case no.	GDNA copy	mRNA expression
1	1.58	23.26
2	1.88	11.09
3	2.06	45.89
4	2.25	17.30
5	2.33	126.80
6	2.33	67.17
7	2.79	1.42
8	2.86	0.79
9	2.89	3.49
10	3.01	5.90
11	3.10	1,299.55
12	3.24	10.90
13	3.41	176.49
14	3.42	244.26
15	4.37	303.09
16	5.64	73.48
17	5.74	115.91
18	5.82	242.87
19	7.00	468.99
20	16.24	9,752.70

Subchromosomal deletion and loss of heterozygosity in CCCs. One of the advantages of high-density SNP array is its exquisitely sensitive resolution that allows for the detection of discrete subchromosomal deletion. By using affinity-purified tumor cells, we were able to detect discrete homozygous deletions that have not been previously described. These include deletions at chr2q12.1, chr8p21.3, and chr9p21.3 (Fig. 3), each of which was identified in one of the 12 fresh samples analyzed. One additional case with copy neutral loss of heterozygosity (LOH) was identified in the chr2q12.1 and chr9p21.3 locus, respectively, but not in the chr8p21.3 locus. The deletion at chr2q12.1 encompasses 104,649,000 to 109,476,000 bp and harbors at least 25 known genes. There is no known tumor suppressor gene reported thus far in this region. Deletion at chr8p21.3 spans from 19,651,900 to 21,642,400 bp and includes *leucine zipper, putative tumor suppressor 1* (*LZTS1*), a previously reported candidate tumor suppressor gene. The frequency of homozygous deletion at *LZTS* locus is low because it is only identified in 1 of 12 cases by SNP array analysis and in 1 of 21 additional cases analyzed by qPCR. Deletion at chr9p21.3 spans from 21,596,500 to 22,009,700 bp at chromosome 9 and includes a well-known tumor suppressor gene, *CDKN2A/2B*. Based on qPCR analysis in 21 additional cases of affinity-purified CCCs, we detected homozygous deletions of this locus in two of the samples, making a total homozygous deletion frequency of 9% (3 of 33 cases). Mutational analysis

of the *CDKN2A/2B* gene failed to show somatic mutations in any of the 12 CCCs examined.

There were no subchromosomal deletions observed in chr1; however, we found two cases harboring copy neutral LOH at chr1p36.22 (Fig. 3). Our previous report has shown frequent hemizygous deletions and LOH in this region in low-grade ovarian serous tumors (16).

Copy number alterations in CCC cell lines. In addition to the 12 CCC tissue samples, we performed the same SNP array analysis using genomic DNA isolated from 10 CCC cell lines that were used in our previous study for mutational analysis of *PIK3CA* (16). Although our previous report showed a similar mutation frequency of *PIK3CA* between affinity-purified clinical CCC samples and cell lines, surprisingly, the DNA copy number alterations and LOH in the cell lines were very different from that detected in the CCC clinical samples (Supplementary Fig. S2; Fig. 4). For example, *ZNF217* amplification was only observed in 1 of 10 CCC cell lines in contrast to 5 of 12 clinical CCC samples (Fig. 2A). In clinical samples, the CIN indices at chromosomes 6, 11, 13, and 18 approached zero, whereas those in CCC cell lines were significantly elevated ($P < 0.05$, Mann-Whitney test; Fig. 4B). Furthermore, the deletions detected in clinical samples were not the same as those

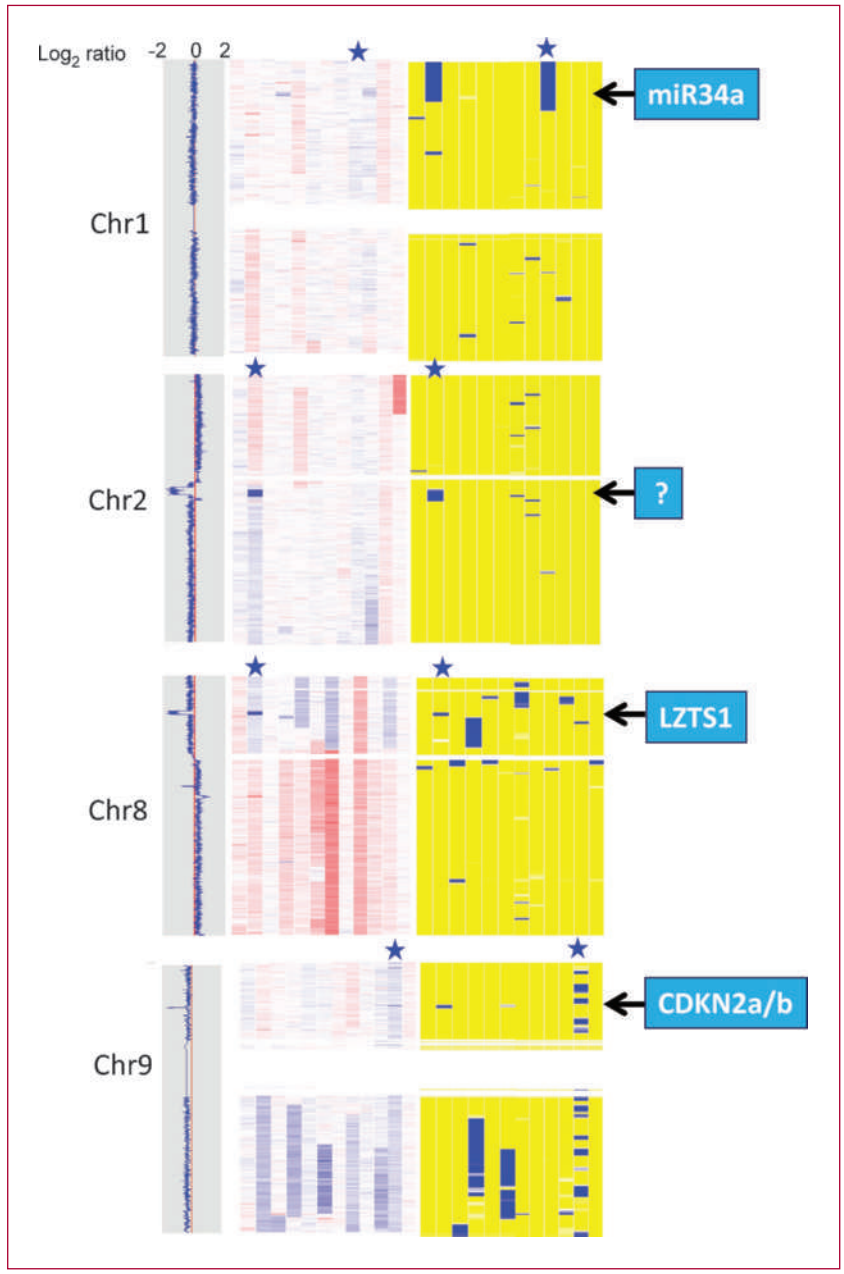

Fig. 3. Copy number alteration in chromosome 1, 2, 8, and 9. DNA copy number changes are represented as pseudocolor gradients corresponding to the copy number increase (red boxes) and decrease (blue boxes) compared with pooled normal samples. LOHs are represented as pseudocolor; blue, LOH; yellow, non-LOH. ★, tumor with DNA copy number tracing plotted at the left. Arrows, candidate tumor suppressor genes residing within the deleted or LOH regions.

detected in the cell lines except for the *CDKN2A/B* locus. In contrast, many amplifications, deletions, and LOHs were found only in cell lines but not in clinical specimens (Supplementary Fig. S2; Fig. 4). A list of the amplifications and deletions detected in CCC cell lines appears in Supplementary Tables S3 and S4.

Growth inhibition by ZNF217 siRNA in CCCs. Given the frequent amplification at the chr20q13.2 locus and the overexpression of ZNF217 in CCCs, we decided to examine if ZNF217 is required for the oncogenesis in CCCs. OVMANA, a CCC cell line that harbored *ZNF217* amplification and overexpression, and OV207, a CCC line with ZNF217 overexpression were selected for functional studies (Fig. 5). The relative ZNF217 mRNA levels decrease to 45% in OVMANA and 35% in OV207 compared with control (luciferase) siRNA after treatment of ZNF217

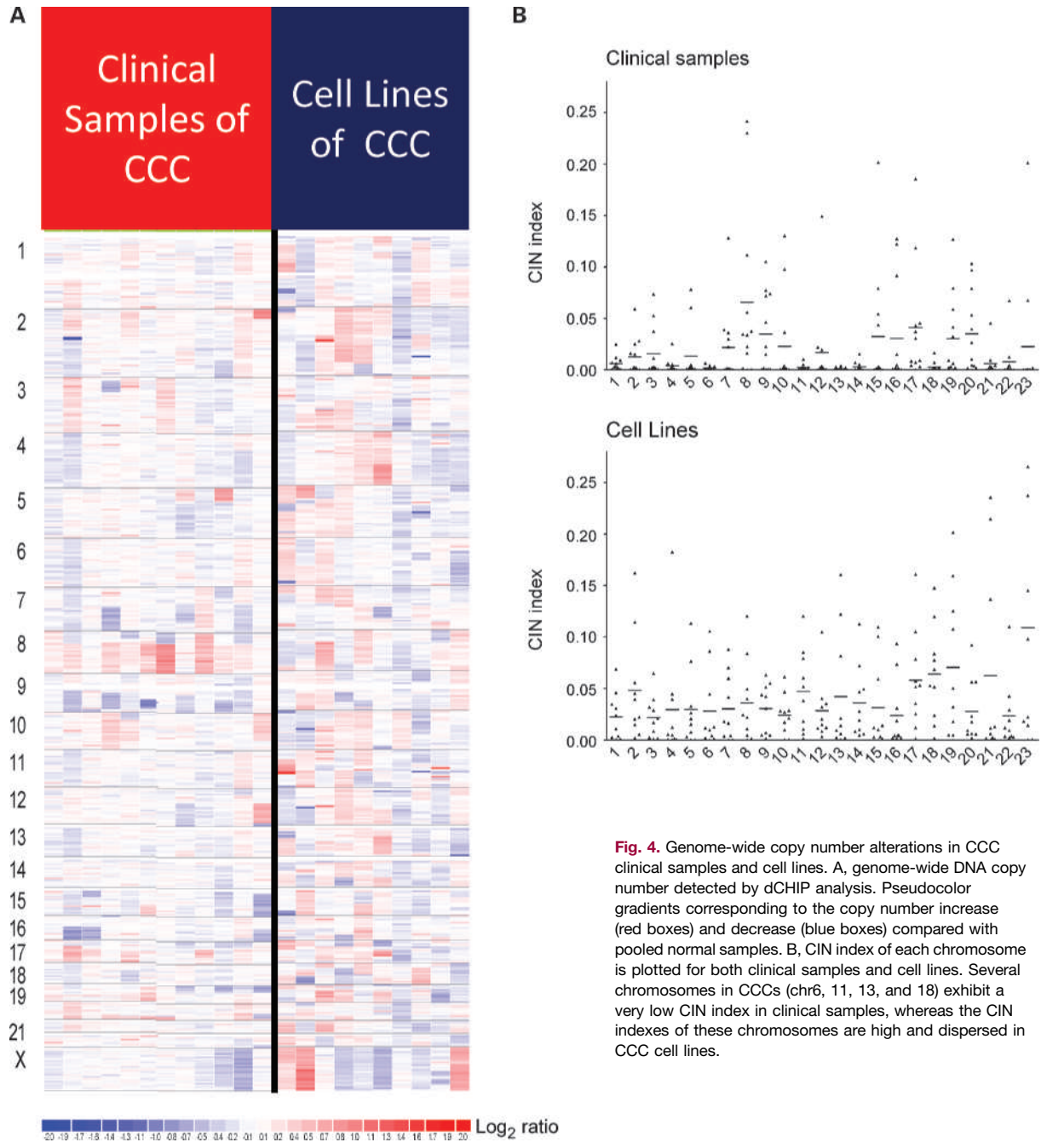

Fig. 4. Genome-wide copy number alterations in CCC clinical samples and cell lines. A, genome-wide DNA copy number detected by dCHIP analysis. Pseudocolor gradients corresponding to the copy number increase (red boxes) and decrease (blue boxes) compared with pooled normal samples. B, CIN index of each chromosome is plotted for both clinical samples and cell lines. Several chromosomes in CCCs (chr6, 11, 13, and 18) exhibit a very low CIN index in clinical samples, whereas the CIN indexes of these chromosomes are high and dispersed in CCC cell lines.

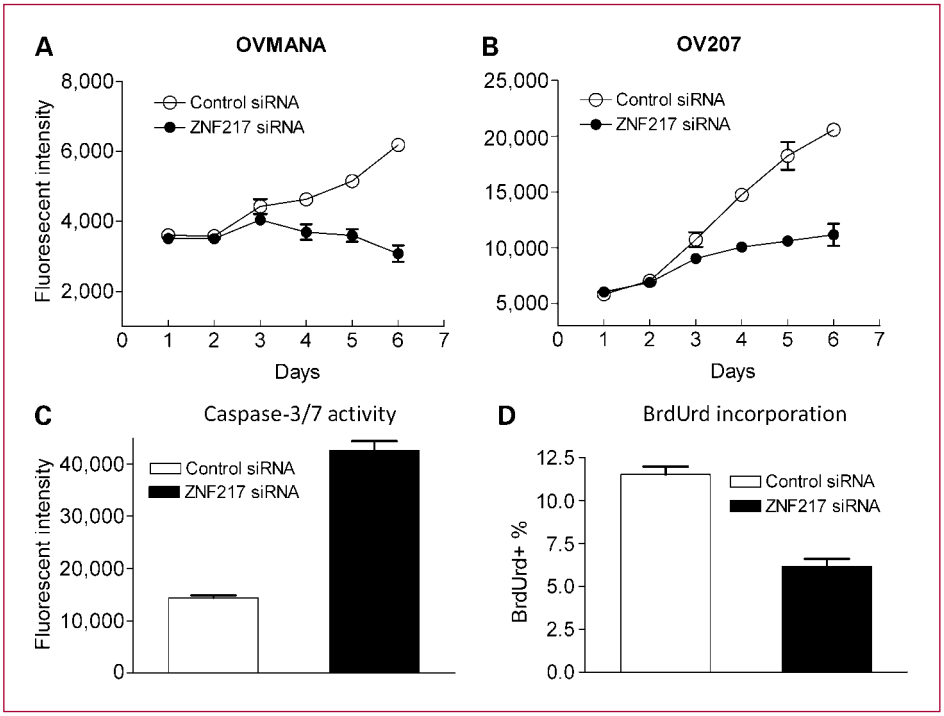

Fig. 5. Biological effects of ZNF217 siRNA in CCC cell lines. A and B, growth curve analysis shows that treatment of ZNF217 siRNA inhibits cell growth in both OVMANA and OV207 lines. C, ZNF217 siRNA treatment induces apoptosis based on the Caspase-3/7 Glo assay. D, ZNF217 siRNA treatment suppresses BrdUrd incorporation as determined by immunostaining using an BrdUrd-specific antibody. C and D, data from 72 h after siRNA treatment in OV207.

siRNA (Supplementary Fig. S3), and significantly suppressed cell growth in CCC cell lines (Fig. 5A and B). We then used OV207 as a representative cell line to determine if the reduced cell number is due to a decrease in cellular proliferation and/or an increase in apoptosis. We found that ZNF217 siRNA treatment resulted in a significantly higher caspase-3/7 activity in CCC cells than the control group treated with luciferase siRNA (*t* test, $P < 0.01$). Moreover, we also observed that the cells with BrdUrd incorporation significantly decreased by ZNF217 siRNA compared with luciferase siRNA ($P < 0.01$; Fig. 5C and D).

Discussion

This is the first study analyzing the ovarian CCC genome using high-density SNP arrays on affinity-purified tumor samples. Our approach offers the assessment of genome-wide DNA copy number alterations in CCCs with very high resolution because affinity purification minimizes contamination by stromal and inflammatory cells that may mask small discrete amplifications and homozygous deletions. Our data show that the level of CIN in CCC is significantly lower than that seen in high-grade serous carcinomas. Moreover, we identified discrete regions with either DNA copy number gain or loss with a resolution level that was never achieved. Lastly, we found evidence that CCC cell lines are distinctly different from fresh CCC tissues in their DNA copy number landscapes, attesting to the fact that many established cell lines have been selected through passages *in vitro* and may not represent their *in vivo* counterparts. We believe the information provided by this study has many important biological and clinical implications.

Among the amplified regions detected, the only one with a discrete amplicon with >2-fold amplification is located at chr20q13.2 containing three genes: *TSHZ2*, *BCAS1*, and *ZNF217*. The amplification occurs in up to 36% of CCCs, suggestive of an important role of this amplicon in CCC development. *Teashirt zinc finger homeobox 2* (TSHZ2) encodes a zinc finger protein, and its homologue in *Drosophila* is involved in the specification of the embryonic trunk (27). It was also known as the ovarian cancer–related protein, indicating its abundant expression in ovarian cancer. *Breast carcinoma–amplified sequence 1* (*BCAS1*) was previously identified as a gene within the 20q13 amplicon (28). However, this gene is located at the border of the amplicon and its expression was not detected in the breast cancer cell line, MCF7, in which this region is highly amplified (28). *Zinc finger protein 217* (*ZNF217*) encodes a nuclear protein with Krüppel-like zinc finger domains and serves as a common protein in forming transcriptional repressor complexes with containing *HDAC2* and *LSD1* (29, 30). Previous reports have shown frequent amplification and overexpression of *ZNF217* in other carcinomas including breast, colorectal, and prostate. The amplification frequency was found to range from 10% to 50% in these tumors (26, 31–34). In breast carcinomas, increased *ZNF217* expression was found to be associated with a poor prognosis and ectopic expression of *ZNF217*-immortalized epithelial cells, and resulted in the loss of transforming growth factor-β responsiveness (35). In this study, we found a significant correlation of genomic DNA and mRNA copy numbers

of ZNF217 in CCC samples. Furthermore, like in other cancer types (36, 37), we showed the essential role of ZNF217 in maintaining cellular proliferation and survival, an observation further supporting a role for *ZNF217* in CCC tumorigenesis.

Among different types of ovarian carcinomas, discrete amplification of the *ZNF217* locus seems specific to CCCs, as our previous SNP analysis in serous ovarian tumors has identified DNA copy number gain of the entire or large region of chr20q arm rather than a relative minute amplicon (22). Although we have only analyzed 33 CCCs thus far, there seems to be no statistically significant difference in the rate of *ZNF217* amplification between early stage (stage I) and advanced stage (III and IV; $P > 0.05$).

In this study, we detected homozygous deletions at three different loci in CCCs. The first one is at 9p21.3 that harbors the *CDKN2A/2B* gene. The homozygous deletion frequency at the *CDKN2A/2B* locus is ~9%. Deletion at the chr9p region encompassing *CDKN2A/2B* has been detected by CGH in 17% to 55% of CCCs (38–40). Our results confirm loss of this locus containing *CDKN2A/2B* in a significant number of CCC cases and implicate its role in the pathogenesis of CCC. Two other novel discrete homozygous deletions at chr2q12.1 and chr8p21.3 were also identified by us. The deleted locus at chr2q12.1 includes >25 genes in which the candidate tumor suppressor(s) is currently not known and will require further investigation. The deleted locus at chr8p21.3 contains a candidate tumor suppressor gene *leucine zipper, putative tumor suppressor-1* (*LZTS1*). *LZTS1* encodes a transcription factor that contains the leucine zipper motif and, when reintroduced into Lzts1-null cancer cells, it suppresses cell growth (41, 42). A recent study has shown that Lzts1 knockout mice are prone to develop spontaneous tumors and, furthermore, mouse embryonic fibroblasts from these animals display increased mitotic progression, decreased Cdk1 activity, and are resistant to Taxol- and Nocodazole-induced M-phase arrest (43). These findings may explain the long-time clinical observation that CCCs are resistant to conventional chemotherapeutic drugs such as Taxol.

Another observation in this study is that CCC cell lines harbor a genomic landscape distinct from that identified in fresh CCC tissues. For example, *ZNF217* amplification was found in 36% of the 33 clinical samples as opposed to only 1 (10%) of the 10 CCC cell lines analyzed. In addition, we found that CCC cell lines do not have the high-frequency DNA copy number gain at 8q that is observed in CCC tissues nor do they contain deletions seen in CCC tissues except for *CDKN2A/2B*. On the other hand, CCC cell lines harbor many genomic alterations that are not detected in the clinical samples, making interpretation of their biological and clinical implications difficult. It should be noted that we used the same genomic DNA preparation of these CCC clinical samples and cell lines in a previous mutational analysis study (16), which interestingly we observed similar frequencies of somatic *PIK3CA* mutation in CCC tissues (45%) and CCC cell lines (40%). One explanation for this disparate finding is that different selection pressures exist under *in vivo* and *in vitro* conditions for different types of mutation. It is possible that point mutation of *PIK3CA* and deletion of *CDKN2A/2B* confer a survival advantage for both tumor cells *in vivo* and those maintained *in vitro* as immortalized cell lines, whereas amplification of *ZNF217*, among other DNA copy number changes, is advantageous only to tumor cells *in vivo*. If this is true, our observations add to many previous reports that cautions should be taken in interpreting the results of DNA copy number alterations identified only in cell lines. Another observation in this study is that we did not detect increased DNA copy numbers in either *PIK3CA* or *AKT* locus in all CCCs. This finding together with our previous study showing frequent *PIK3CA* mutation suggest that activating *PIK3CA* mutation represents the major mechanism in eliciting PIK3CA/AKT pathway in CCCs.

A dualistic model of ovarian carcinogenesis based on clinicopathologic and molecular genetic studies has been proposed for ovarian carcinomas (44–46). In this model, low-grade serous, mucinous, and endometrioid carcinomas are designated as "type I" tumors. These neoplasms develop in a stepwise fashion from well-recognized precursors termed "borderline" tumors that originate from cystadenomas/adenofibromas and endometriosis. They typically are low-grade, present as large cystic tumors confined to the ovary, and have an indolent behavior. In contrast, high-grade serous carcinoma, undifferentiated carcinoma, and malignant mixed mesodermal tumors (carcinosarcomas) are designated as "type II" tumors. In contrast to type I tumors, these high-grade malignancies are not associated with benign precursor lesions at pathologic evaluation. Recent studies have suggested that type II tumors develop from high-grade intraepithelial carcinomas in the fimbriated portion of the fallopian tube. Regardless of their origins, type II tumors are invariably highly aggressive and the disease often is in advanced stages at the time of diagnosis. Compared with type I tumors at the molecular level, type II tumors have high chromosome instability and are characterized by frequent *TP53* mutations. In contrast, type I tumors have moderate chromosome instability and contain frequent somatic mutations of genes participating in signal transduction pathways, including *KRAS/BRAF*, *PTEN/PIK3CA*, and *CTNNB1*. In contrast, mutational analysis indicates that these genes are rarely mutated in type II tumors.

CCC appears to exhibit features of both type I and type II neoplasms. Similar to type I tumors, CCCs develop from well-characterized benign precursors (e.g., endometriosis) and present as large cystic tumors confined to the ovary. However, when the disease spreads beyond the ovary, CCC is typically high-grade, high-staged, and very aggressive. CCC was tentatively assigned to the type I group awaiting the results of molecular genetic studies that could assist in its more accurate categorization. In this study, we found that CCCs have a CIN index very

similar to that of low-grade serous carcinomas and much lower than that of high-grade serous carcinomas. This finding together with our previous results showing rare *TP53* mutations but frequent *PIK3CA*-activating mutations in CCCs (16) are in stark contrast to results obtained in high-grade serous carcinomas and strongly support classifying CCC as a type I tumor.

In summary, this is the first report describing DNA copy number changes in the CCC genome using high-density SNP array analysis of purified tumor cells isolated from fresh cancerous tissue. Based on the CIN index of CCCs analyzed and their previously reported mutational profiles, CCC is much more similar to type I tumors at the molecular level than to type II tumors. Our current analysis also identified novel amplification and deletion in CCC. The frequent amplification of the *ZNF217* locus and deletion of the *CDKN2A/2B* locus suggest that pathways involving these two genes are important in CCC tumorigenesis. We believe that the analysis of CCCs described herein is a snapshot of the genomic landscape of this disease and provide a very useful foundation for future studies aimed at elucidating the molecular pathogenesis of CCC and at the development of target-based therapeutics for this highly aggressive ovarian malignancy.

Disclosure of Potential Conflicts of Interest

No potential conflicts of interest were disclosed.

Grant Support

U.S. Department of Defense Research Council OC0400600 (T-L. Wang), American Cancer Society RSG-08-174-01-GMC (T-L. Wang), Ovarian Cancer Research Fund (T-L. Wang), NIH RO1CA116184 (R.J. Kurman), NIH RO1CA129080 (I-M. Shih), NIH RO1 R01CA103937 (I-M. Shih), NSC97-2320-B-002-047-MY3 (T.-L. Wang), and NIH R33CA109872 (Y. Wang).

The costs of publication of this article were defrayed in part by the payment of page charges. This article must therefore be hereby marked *advertisement* in accordance with 18 U.S.C. Section 1734 solely to indicate this fact.

Received 08/05/2009; revised 12/23/2009; accepted 01/25/2010; published OnlineFirst 03/16/2010.

References

1. Cho KR, Shih IM. Ovarian cancer. Annu Rev Pathol Mech Dis 2009;4:287–313.
2. Seidman JD, Russell P, Kurman RJ. Surface epithelial tumors of the ovary. In: Kurman RJ, editor. Blaustein's Pathology of the Female Genital Tract. 5th ed. New York: Springer Verlag; 2002, p. 791–904.
3. Scully RE. World Health Organization International Histological Classification of Tumours. 2nd ed. New York (NY): Springer; 1999.
4. Scully RE. International histological classification of tumors: Histological typing of ovarian tumors. Geneva: World Health Organization; 1999.
5. Veras E, Mao TL, Ayhan A, et al. Cystic and adenofibromatous clear cell carcinomas of the ovary: distinctive tumors that differ in their pathogenesis and behavior: a clinicopathologic analysis of 122 cases. Am J Surg Pathol 2009;33:844–53.
6. Fukunaga M, Nomura K, Ishikawa E, Ushigome S. Ovarian atypical endometriosis: its close association with malignant epithelial tumours. Histopathology 1997;30:249–55.
7. Erzen M, Rakar S, Klancnik B, Syrjanen K. Endometriosis-associated ovarian carcinoma (EAOC): an entity distinct from other ovarian carcinomas as suggested by a nested case-control study. Gynecol Oncol 2001;83:100–8.
8. Takano M, Kikuchi Y, Yaegashi N, et al. Clear cell carcinoma of the ovary: a retrospective multicentre experience of 254 patients with complete surgical staging. Br J Cancer 2006;94:1369–74.
9. Mizuno M, Kikkawa F, Shibata K, et al. Long-term follow-up and prognostic factor analysis in clear cell adenocarcinoma of the ovary. J Surg Oncol 2006;94:138–43.
10. Chan JK, Teoh D, Hu JM, Shin JY, Osann K, Kapp DS. Do clear cell ovarian carcinomas have poorer prognosis compared to other epithelial cell types? A study of 1411 clear cell ovarian cancers. Gynecol Oncol 2008;109:370–6.
11. Pectasides D, Fountzilas G, Aravantinos G, et al. Advanced stage clear-cell epithelial ovarian cancer: the Hellenic Cooperative Oncology Group experience. Gynecol Oncol 2006;102:285–91.
12. Goff BA, Sainz de la Cuesta R, Muntz HG, et al. Clear cell carcinoma of the ovary: a distinct histologic type with poor prognosis and resistance to platinum-based chemotherapy in stage III disease. Gynecol Oncol 1996;60:412–7.
13. Sugiyama T, Kamura T, Kigawa J, et al. Clinical characteristics of clear cell carcinoma of the ovary: a distinct histologic type with poor prognosis and resistance to platinum-based chemotherapy. Cancer 2000;88:2584–9.
14. Crotzer DR, Sun CC, Coleman RL, Wolf JK, Levenback CF, Gershenson DM. Lack of effective systemic therapy for recurrent clear cell carcinoma of the ovary. Gynecol Oncol 2007;105:404–8.
15. Takano M, Sugiyama T, Yaegashi N, et al. Low response rate of second-line chemotherapy for recurrent or refractory clear cell carcinoma of the ovary: a retrospective Japan Clear Cell Carcinoma Study. Int J Gynecol Cancer 2008;18:937–42.
16. Kuo KT, Mao TL, Jones S, et al. Frequent activating mutations of PIK3CA in ovarian clear cell carcinoma. Am J Pathol 2009;174:1597–601.
17. Shih Ie M, Wang TL. Apply innovative technologies to explore cancer genome. Curr Opin Oncol 2005;17:33–8.
18. Lau KM, Mok SC, Ho SM. Expression of human estrogen receptor-α and -β, progesterone receptor, and androgen receptor mRNA in normal and malignant ovarian epithelial cells. Proc Natl Acad Sci U S A 1999;96:5722–7.
19. Shaw TJ, Senterman MK, Dawson K, Crane CA, Vanderhyden BC. Characterization of intraperitoneal, orthotopic, and metastatic xenograft models of human ovarian cancer. Mol Ther 2004;10:1032–42.
20. Garson K, Shaw TJ, Clark KV, Yao DS, Vanderhyden BC. Models of ovarian cancer—Are we there yet? Mol Cell Endocrinol 2005;239:15–26.
21. Nakayama K, Nakayama N, Jinawath N, et al. Amplicon profiles in ovarian serous carcinomas. Int J Cancer 2007;120:2613–7.
22. Kuo KT, Guan B, Feng Y, et al. Analysis of DNA copy number alterations in ovarian serous tumors identifies new molecular genetic changes in low-grade and high-grade carcinomas. Cancer Res 2009;69:4036–42.
23. Wang TL, Maierhofer C, Speicher MR, et al. Digital karyotyping. Proc Natl Acad Sci U S A 2002;99:16156–61.
24. Buckhaults P, Zhang Z, Chen YC, et al. Identifying tumor origin using a gene expression-based classification map. Cancer Res 2003;63:4144–9.
25. Letessier A, Sircoulomb F, Ginestier C, et al. Frequency, prognostic impact, and subtype association of 8p12, 8q24, 11q13, 12p13, 17q12, and 20q13 amplifications in breast cancers. BMC Cancer 2006;6:245.
26. Weiss MM, Snijders AM, Kuipers EJ, et al. Determination of amplicon boundaries at 20q13.2 in tissue samples of human gastric

adenocarcinomas by high-resolution microarray comparative genomic hybridization. J Pathol 2003;200:320–6.
27. Caubit X, Tiveron MC, Cremer H, Fasano L. Expression patterns of the three Teashirt-related genes define specific boundaries in the developing and postnatal mouse forebrain. J Comp Neurol 2005; 486:76–88.
28. Collins C, Rommens JM, Kowbel D, et al. Positional cloning of ZNF217 and NABC1: genes amplified at 20q13.2 and overexpressed in breast carcinoma. Proc Natl Acad Sci U S A 1998;95:8703–8.
29. Cowger JJ, Zhao Q, Isovic M, Torchia J. Biochemical characterization of the zinc-finger protein 217 transcriptional repressor complex: identification of a ZNF217 consensus recognition sequence. Oncogene 2007;26:3378–86.
30. Hakimi MA, Dong Y, Lane WS, Speicher DW, Shiekhattar R. A candidate X-linked mental retardation gene is a component of a new family of histone deacetylase-containing complexes. J Biol Chem 2003;278:7234–9.
31. Nancarrow DJ, Handoko HY, Smithers BM, et al. Genome-wide copy number analysis in esophageal adenocarcinoma using high-density single-nucleotide polymorphism arrays. Cancer Res 2008;68:4163–72.
32. Tanner MM, Grenman S, Koul A, et al. Frequent amplification of chromosomal region 20q12-13 in ovarian cancer. Clin Cancer Res 2000;6:1833–9.
33. Suzuki S, Egami K, Sasajima K, et al. Comparative study between DNA copy number aberrations determined by quantitative microsatellite analysis and clinical outcome in patients with stomach cancer. Clin Cancer Res 2004;10:3013–9.
34. Quinlan KG, Verger A, Yaswen P, Crossley M. Amplification of zinc finger gene 217 (ZNF217) and cancer: when good fingers go bad. Biochim Biophys Acta 2007;1775:333–40.
35. Nonet GH, Stampfer MR, Chin K, Gray JW, Collins CC, Yaswen P. The ZNF217 gene amplified in breast cancers promotes immortalization of human mammary epithelial cells. Cancer Res 2001;61: 1250–4.
36. Huang G, Krig S, Kowbel D, et al. ZNF217 suppresses cell death associated with chemotherapy and telomere dysfunction. Hum Mol Genet 2005;14:3219–25.
37. Li P, Maines-Bandiera S, Kuo WL, et al. Multiple roles of the candidate oncogene ZNF217 in ovarian epithelial neoplastic progression. Int J Cancer 2007;120:1863–73.
38. Suehiro Y, Sakamoto M, Umayahara K, et al. Genetic aberrations detected by comparative genomic hybridization in ovarian clear cell adenocarcinomas. Oncology 2000;59:50–6.
39. Kiechle M, Jacobsen A, Schwarz-Boeger U, Hedderich J, Pfisterer J, Arnold N. Comparative genomic hybridization detects genetic imbalances in primary ovarian carcinomas as correlated with grade of differentiation. Cancer 2001;91:534–40.
40. Dent J, Hall GD, Wilkinson N, et al. Cytogenetic alterations in ovarian clear cell carcinoma detected by comparative genomic hybridisation. Br J Cancer 2003;88:1578–83.
41. Ishii H, Baffa R, Numata SI, et al. The FEZ1 gene at chromosome 8p22 encodes a leucine-zipper protein, and its expression is altered in multiple human tumors. Proc Natl Acad Sci U S A 1999;96:3928–33.
42. Ishii H, Vecchione A, Murakumo Y, et al. FEZ1/LZTS1 gene at 8p22 suppresses cancer cell growth and regulates mitosis. Proc Natl Acad Sci U S A 2001;98:10374–9.
43. Vecchione A, Baldassarre G, Ishii H, et al. Fez1/Lzts1 absence impairs Cdk1/Cdc25C interaction during mitosis and predisposes mice to cancer development. Cancer Cell 2007;11:275–89.
44. Shih I-M, Kurman RJ. Ovarian tumorigenesis—a proposed model based on morphological and molecular genetic analysis. Am J Pathol 2004;164:1511–8.
45. Shih Ie M, Kurman RJ. Molecular pathogenesis of ovarian borderline tumors: new insights and old challenges. Clin Cancer Res 2005;11: 7273–9.
46. Kurman RJ, Visvanathan K, Roden R, Wu TC, Shih Ie M. Early detection and treatment of ovarian cancer: shifting from early stage to minimal volume of disease based on a new model of carcinogenesis. Am J Obstet Gynecol 2008;198:351–6.